MECHANOCHEMISTRY AND MECHANICAL ALLOYING 2003

JOURNAL OF MATERIALS SCIENCE **39** (2004) 5213–5216

Mechanically driven decomposition of intermetallics

YOUNG-SOON KWON, JI-SOON KIM, DONG-WOOK CHOI
Regional Research Center, ReMM, School of Materials Science and Engineering, University of Ulsan, Ulsan, 680-749, South Korea

K. B. GERASIMOV*, S. S. AVRAMCHUCK
Institute of Solid State Chemistry and Mechanochemistry, Kutateladze 18, Novosibirsk 128, 630128 Russia
E-mail: rrc@uou.ulsan.ac.kr; gerasimov@solid.nsk.su

Under mechanical milling (MM) in a planetary ball mill the FeSn intermetallic decomposes with the formation of the Fe_5Sn_3 and $FeSn_2$ phases, and the Fe_2Ge_3 decomposes into FeGe (B20) and $FeGe_2$. These processes were investigated using X-ray diffraction (XRD), and magnetization measurements in order to assess whether or not local melting upon impact by milling balls, or low-temperature solid-state processes are responsible for decomposition. Fe_2Ge_3 decomposes completely after a relatively short milling period, while the amount FeSn decomposed reaches a steady state, depending on milling conditions, after prolonged milling. Particle sizes of the decomposition products (Fe_5Sn_3 and FeGe) determined from the XRD and magnetization data remain approximately constant during MM. These peculiarities are in good accordance with local melting as a mechanism of the mechanical decomposition of FeSn and Fe_2Ge_3. © *2004 Kluwer Academic Publishers*

1. Introduction

The mechanically driven decomposition of intermetallics is, probably, the most inscrutable phenomenon observed for MM. Obviously, the compounds, which decompose during MM, cannot be obtained as a single-phase homogeneous product of mechanical alloying (MA), at least under the same milling conditions. Therefore, an ascertainment of the nature of processes, which underlay the mechanical decomposition of intermetallics, is necessary to formulate a predictive model of MA.

Loeff and Bakker [1] first observed the decomposition of intermetallics due to high-energy ball milling. According to their data, some La-based intermetallics decomposed into f.c.c. β-lanthanum and other elemental components. However, further and deeper inspection showed that the f.c.c. phase was not pure lanthanum but LaN [2]. In this case, the mechanical decomposition turned up a reaction with nitrogen impurities in a protective atmosphere. The reason for the decomposition of intemetallics in the Zr-Co and Ti-Cu system under MM in Ref. [3] may be similar. Either the Zr_3Co or $TiCu_4$ phases were always observed in the decomposition products; and these phases were stabilized by oxygen.

However, there are other examples of mechanical decompositions, which are not simply explained by contamination effects. The decomposition of the $Nd_2Fe_{14}B$ and related compounds, first observed by Alonso *et al.* [4], was reproduced in a number of other studies concerning the synthesis of nanocomposite magnets. The work [5] indicated that the Sm_2Fe_{17} decomposes under MM into a mixture of an amorphous and α-Fe phase. The decomposition of the FeSn intermetallic was observed for MM [6–8]. Tang *et al.* [9, 10] observed the decomposition of the $NdFe_{11}Ti$ and $Nd_3(Fe, Ti)_{29}$ intermetallics into an amorphous phase and α-Fe(Ti). Kwon *et al.* [11] recently reported the decomposition of the Fe_6Ge_5 intermetallic into the β-$Fe_{2-x}Ge$ and the cubic B20 polymorph of FeGe; and the decomposition of the Fe_2Ge_3 with the formation of the $FeGe_2$ and FeGe (B20) phases. Except the decomposition caused by contamination effects [1, 3], all intermetallics, which decompose under MM, are incongruently melting compounds. So the mechanical decomposition of intermetallics may be attributed to local melting under ball collisions [6, 11].

In this paper, the decomposition of the FeSn and Fe_2Ge_3 intermetallics was comparatively studied. The aim of the investigation was to gain an understanding of the separation process and to assess whether the local melting under pressure and temperature pulses, generated upon impact by milling balls, or low-temperature solid-state processes were responsible for the decomposition of these intermetallics during MM in high-energy ball mills.

---

*Author to whom all correspondence should be addressed.

2. Experimental

To reduce the influence of surface oxides, coarse powders of Fe (99.9% purity), Ge (semiconductor grade) and Sn (99.99%) were used in this study. MM was performed in an AGO-2 planetary ball mill with hardened steel balls and vials. Before milling the vials were evacuated and filled by hydrogen with a pressure of 0.5 MPa to reduce the temperature of the milling balls [12]. The ball charge was approximately 200 g and the mass of the powders being treated was 10 g in each vial.

For preparation of the intermetallics, powder blends with corresponding compositions were initially milled for 30 min and after that annealed in an inert atmosphere during some days at 780 K for the Fe_2Ge_3 and during 10 h at 970 K for the FeSn. The samples were examined by powder X-ray diffraction (XRD) using Co K_α and Fe K_α radiation. Magnetization curves were obtained by using a vibrating sample magnetometer with a maximum applied field of 17.3 kOe.

The usual procedure to check for contamination was to anneal the milled samples at 673 K during 1 h under inert atmosphere to restore the original properties of the sample. We checked both phase composition and magnetic properties. Since the FeSn has a small homogeneity range and all the phases of the Fe-Sn system with an iron content higher than in FeSn are ferromagnetic [13], the magnetic properties have been especially sensitive to iron contamination. For the Fe_2Ge_3, the situation was similar. The adjacent compound having a higher iron content was the FeGe. The low-temperature B20 polymorph of this phase, which is stable until 900 K, orders magnetically at $T_N = 278.7$ K into a very-long-range spiral [14]. An applied magnetic field of 2–3 kOe causes the amplitude of the antiferromagnetic spiral to decrease to zero and the compound becomes ferromagnetic magnetically saturated [14, 15]. So the small magnetization of the milled samples after annealing was a direct confirmation of negligible iron contamination for both the FeSn and Fe_2Ge_3 intermetallics.

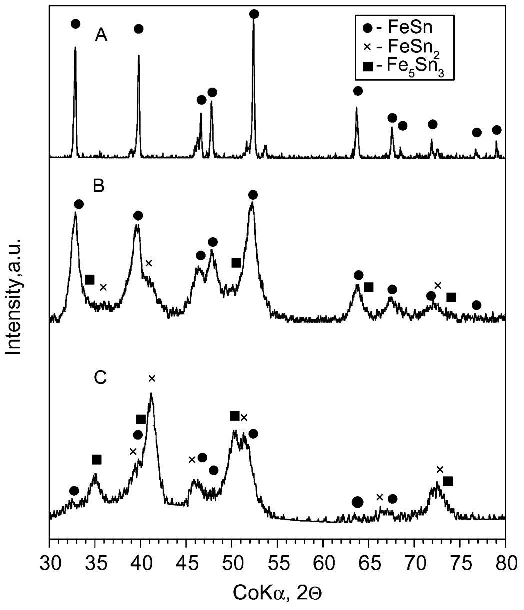

Figure 1 XRD patterns of FeSn intermetallic: (A) before MM, (B) after 10-min MM with 5.5-mm balls, and (C) after 90-min milling with 5.5-mm balls.

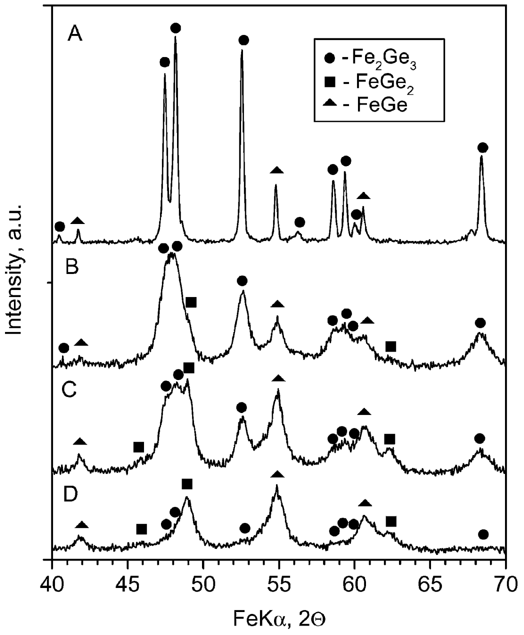

Figure 2 XRD patterns of Fe_2Ge_3–5%FeGe alloy: (A) before MM, (B) after 8-min MM with 5.5-mm balls, (C) after 20-min MM with 5.5-mm balls, and (D) after 30-min milling with 5.5-mm balls.

3. Results

Fig. 1 shows XRD patterns for the initial FeSn and for this intermetallic after MM. It can be seen, that the FeSn decomposed under MM into Fe_5Sn_3 and $FeSn_2$ phases. The fitting of the XRD-patterns with the Powder Cell 2.3 program provided information about the amount of the phases in the milled powders and the average grain size for these phases. The grain sizes were approximately equal to 10 nm for all phases, and only slightly changed with milling time and milling conditions. The fraction of FeSn decomposed was determined from the part of this phase in the milled powders.

Fig. 2 shows the XRD-patterns for the initial alloy, which had the composition Fe_2Ge_3–95% and FeGe (B20)–5% according to XRD data, and for this alloy after MM. One can see, that the Fe_2Ge_3 decomposed into FeGe (B20) and $FeGe_2$ phases. The dependences of the decomposed fraction on milling time for the FeSn and Fe_2Ge_3 are collated in Fig. 3. The kinetic curve for the decomposition of the Fe_2Ge_3 had a pronounced S-shaped form. After a relatively short milling period the Fe_2Ge_3 decomposed completely. No sign of an acceleration period was found for the decomposition of FeSn. The fraction of FeSn decomposed increased with milling time and reached a steady state after prolonged milling. From Fig. 3 one can see, that the fraction of FeSn decomposed at this steady state is different for different milling conditions: it is larger for smaller milling balls.

Due to an overlapping of XRD peaks from different phases the particle sizes determined from XRD data were not thoroughly reliable, especially for a small fraction of decomposed FeSn. Therefore for a determination of the particle sizes for the Fe_5Sn_3 the procedure described in Refs. [16, 17] was used. The FeSn is an

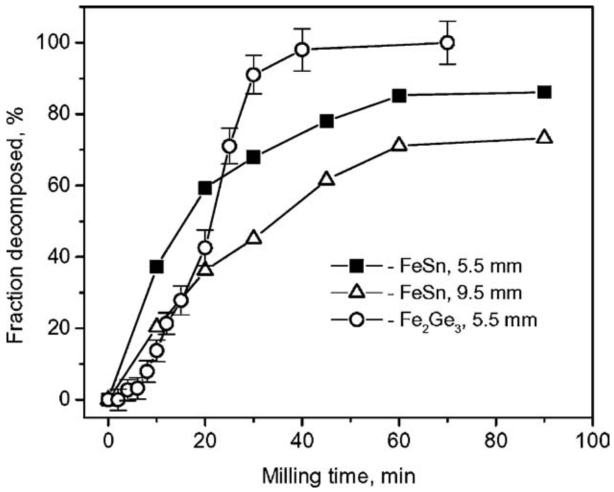

Figure 3 Fraction of FeSn and Fe_2Ge_3 decomposed as a function of milling time. Diameters of milling balls are indicated on inset.

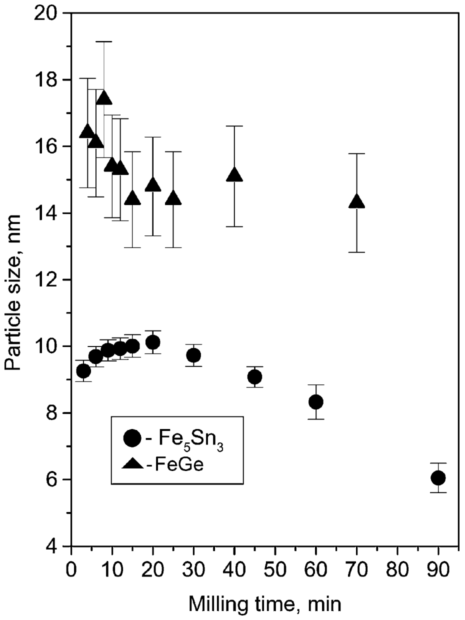

Figure 4 Particle sizes of Fe_5Sn_3 calculated from fitting of magnetization curves and grain sizes of FeGe determined from XRD peaks broadening as a function of milling time.

antiferromagnetic compound ($T_N = 368$ K) and unmilled samples showed only negligible magnetization. One product of the decomposition, $FeSn_2$, is also antiferromagnetic ($T_N = 380$ K) and the other one, Fe_5Sn_3, is ferromagnetic ($T_C = 588$ K) [13]. The milled powders showed considerable magnetization. The specific magnetization of milled powders measured at room temperature with an applied field of 17 kOe was usually 5–10% higher than the magnetization calculated from the decomposition degree and the saturation magnetization of Fe_5Sn_3, $\sigma_s = 90.4$ emu/g [13]. This difference is connected with the contribution in magnetization from FeSn and $FeSn_2$ particles due to an incomplete magnetic compensation in antiferromagnetic nanoparticles. All phases in the milled powder must possess superparamagnetic behavior at an adequately high temperature due to the small grain sizes. The magnetization of the milled FeSn samples with a relatively small decomposition degree shows no hysteresis and the magnetization curves can be fitted by the sum of two Langevin functions. Such a fit allows one to obtain the value of the average magnetic moment and the size of ferromagnetic particles in the system.

Fig. 4 shows the dependence of the mean diameter of Fe_5Sn_3 particles on milling time determined from the magnetization curves. The particle size remained approximately unchanged during the first 30 min of MM. In our opinion, real particle size also changed only slightly with a further increase of milling time and the decrease of calculated size was really connected with a magnetic interaction between the particles in the nanocomposite. Actually, the milled powders with a fraction of FeSn decomposed of more than 60% (when milling time exceeds 30 min) showed hysteric behavior, the magnetization curves in this case cannot be well fitted by a superposition of Langevin functions, and the fitting parameters lose physical meaning.

The Fe_2Ge_3 intermetallic decomposes under MM with the formation of the $FeGe_2$ (C16) and FeGe (B20) phases. The $FeGe_2$ and FeGe (B20) are characterized by complex magnetic properties [14, 15, 18, 19], which were essentially changed under MM. The milled powders of Fe_2Ge_3 showed a very complicated magnetic behavior, and a similar procedure, which was used for an estimation of the grain sizes in the milled powders of FeSn, cannot be used in the case of Fe_2Ge_3. Therefore, for the milled Fe_2Ge_3 powders, the grain sizes of FeGe, which exhibited almost no overlapping with XRD peaks from the other phases, were estimated from the peaks broadening. One can see from Fig. 4, that the particle sizes of FeGe remain approximately constant (within the error of determination) during the MM process.

In order to acquire proof as to whether or not the decomposition of intermetallics is characteristic of the MM itself or whether or not it occurs due to contaminations, the products of MM in each experiment were subjected to annealing under an inert atmosphere at 670 K for 1 h. If the milling time did not exceed 90 min for the FeSn samples and 60 min for the Fe_2Ge_3 samples this annealing was sufficient for a restoration of the initial phase composition and magnetization (the magnetization was measured at 300 K for the FeSn samples and at 220 K for the Fe_2Ge_3 samples).

4. Discussion

Two explanations of the decomposition of FeSn and Fe_2Ge_3 intermetallics during MM are possible. The first is based on the assumption that the local temperature pulses due to ball collisions have a relatively small value. In this case, decomposition should be accounted for by a change in the relative stabilities of the phases in the Fe-Sn and Fe-Ge systems during MM due to a preferential accumulation of defects in the FeSn and Fe_2Ge_3 phases. The decomposition would occur by solid-state diffusion leading to a gradual growth of both particle size and particle number with milling time for the decomposition products, at least for the initial stage of MM.

The second explanation assumes that the temperature pulses during the impaction are sufficient for local melting. Both the FeSn and Fe_2Ge_3 decompose when being heated: the FeSn exhibits peritectic melting at 1034 K [20], while Fe_2Ge_3 shows peritectoid decomposition into FeGe (B20) and $FeGe_2$ at ∼810 K [21]. Several processes should be considered for the decomposition of FeSn. All intermediate compounds of the Fe-Sn system melt incongruently and can decompose under high temperature due to ball collisions. After the collision, the temperature of the melted regions decreased rapidly and reverse processes of intermetallic formation become possible. All these processes must reach a steady state after some time. As a result, the product of MM of FeSn may contain all the phases existing in the Fe-Sn system. Since ball collision generates not only a high local temperature but also a high local pressure, it is reasonable to expect that denser phases should have bigger concentrations. The Fe_5Sn_3 and $FeSn_2$ phases prevailing in MM product have the highest density of all phases in the system [16, 17].

In the case of the decomposition of Fe_2Ge_3, one of the products of decomposition, $FeGe_2$, melts congruently, while another, FeGe (B20), is a low-temperature phase, which is stable below 903 K at normal pressure. The stability of this phase under MM may be attributed to its high density [11]. As in the case of the decomposition of FeSn, the volume change during the decomposition of Fe_2Ge_3 is negative. So local stresses under impaction facilitate the decomposition.

The value and duration of the local temperature pulses depend mostly on the mechanical parameters of the milling balls, their sizes, velocity and so forth [22] and should change only slightly with milling time. This means that, if the decomposition of FeSn and Fe_2Ge_3 occurs due to incongruent melting during impaction of the powder, particle sizes of decomposition products would remain approximately constant during the MM process. Just such a behavior was observed in the present study.

The complete decomposition of Fe_2Ge_3 and the partial decomposition of FeSn as a result of MM may be connected with the higher efficiency of the reverse processes during decreasing of temperatures after collision in the case of FeSn. This reverse process is a peritectic reaction of solid phase (phases) with liquid solution of iron in tin for the FeSn, and the peritectoid reaction between two solid phases for the Fe_2Ge_3. It is reasonably to expect that in the former case the reverse process should be more efficient, leading to a decrease in the decomposition degree and particle sizes for the products.

Thus the result obtained in this work supports the assumption that local melting is possible during the MM process.

5. Conclusion

Under MM the FeSn intermetallic decomposed with formation of Fe_5Sn_3 and $FeSn_2$, and the Fe_2Ge_3 intermetallic decomposed into mixture of FeGe (B20) and $FeGe_2$ phases. According to the results of the XRD and magnetization measurements, the particle sizes of the Fe_5Sn_3 and FeGe (B20) phases remained approximately unchanged during the MM process. The decomposition of FeSn and Fe_2Ge_3 during MM is in good accordance with a model of local melting.

Acknowledgements

This work was supported by 2003 Research Fund of University of Ulsan and also by the Korea Science and Engineering Foundation (KOSEF) through the ReMM at the University of Ulsan, Program No. 02-3-20-8 (invitation program).

References

1. P. I. LOEFF and H. BAKKER, *Europhys. Lett.* **8** (1989) 35.
2. H. BAKKER, G. F. ZHOU and H. YANG, *Progr. Mater. Sci.* **39** (1995) 159.
3. K. B. GERASIMOV, A. A. GUSEV, E. Y. IVANOV and V. V. BOLDYREV, *J. Mater. Sci.* **39** (1991) 2495.
4. T. ALONSO, H. YANG, Y. LIU and P. G. McCORMICK, *Appl. Phys. Lett.* **60** (1992) 833.
5. P. A. I. SMITH and P. G. McCORMICK, *Scr. Met. Mater.* **26** (1992) 485.
6. K. B. GERASIMOV and V. V. BOLDYREV, *Mater. Res. Bull.* **31** (1996) 1297.
7. OU MAO, R. A. DUNLAP and J. R. DAHN, *Solid State Ionics* **118** (1999) 99.
8. OU MAO and J. R. DAHN, *J. Electrochem. Soc.* **146** (1999) 414.
9. S. L. TANG, C. H. WU, B. W. WANG, X. V. JIN, G. S. LI, B. Z. DING and Y. C. CHUANG, *J. Magn. Magn. Mater.* **188** (1998) 387.
10. S. L. TANG, Z. Q. JIN, S. Y. ZHANG and Y. W. DU, *NanoStruct. Mater.* **12** (1999) 705.
11. Y.-S. KWON, K. B. GERASIMOV, O. I. LOMOVSKY and S. V. PAVLOV, *J. Alloys Compd.* **353** (2003) 194.
12. Y.-S. KWON, K. B. GERASIMOV and S.-K. YOON, *ibid.* **346** (2002) 276.
13. G. TRUMPY, E. BOTH, C. DIEGA-MARIADASSOU and P. LECOCQ, *Phys. Rev.* B **2** (1970) 3477.
14. B. LEBECH, J. BERNHARD and T. FRELTOFT, *J. Phys.: Condens. Mater.* **1** (1989) 6105.
15. L. LUNDGREN, K. A. BLOM and O. BECKMAN, *Phys. Lett.* **28A** (1968) 175.
16. Y.-S. KWON, K. B. GERASIMOV, S. S. AVRAMCHUCK and J.-S. KIM, *J. Metast. Nanocryst. Mater.* **15/16** (2003) 301.
17. Y.-S. KWON, K. B. GERASIMOV and S. S. AVRAMCHUCK, *J. Alloys Compd.*, in press.
18. T. E. MASON, C. P. ADAMS, S. A. M. MENTINK, E. FAWCETT, A. Z. MENSHIKOV, C. D. FROST, J. B. FORSYTH, T. G. PERRING and T. M. HOLDEN, *Physica* B **237/238** (1997) 449.
19. L. M. CORLISS, J. M. HASTING, W. KUNNMANN, R. THOMAS, J. ZHUANG, R. BUTERA and D. MUKAMEL, *Phys. Rev.* B **31** (1985) 4337.
20. K. C. HARI KUMAR, P. WOLLANTS and L. DELAYE, *CALPHAD* **20** (1996) 139.
21. K. B. GERASIMOV and S. V. PAVLOV, *Intermetallics* **8** (2000) 451.
22. D. R. MAURICE and T. H. COURTNEY, *Metall. Trans.* **21A** (1990) 289.

Received 11 September 2003
and accepted 27 February 2004